Magma Chamber Dynamics at the Campi Flegrei Caldera, Italy

Chiara P. Montagna, Paolo Papale, and Antonella Longo

Abstract

The Campi Flegrei caldera volcanic system is certainly a remarkable case study of magma chamber dynamics. Its magmatic and volcanic history appears to have been largely driven by magma chamber processes like fractional crystallisation, magma mixing, and volatile degassing. These processes have been intensely investigated with a variety of approaches that are described in many chapters of this book, and more specifically, in Chaps. An Evolutionary Model for the Magmatic System of the Campi Flegrei Volcanic Field (Italy) Constrained by Petrochemical Data; Rheological Properties of the Magmas Feeding the Campi Flegrei Caldera (Italy) and Their Influence on Mixing Processes. In this chapter, physical modelling and numerical simulations are employed in order to study the dynamics of magma convection and mixing in a vertically extended, geometrically complex, compositionally heterogeneous magmatic system representing a schematic simplification of an overall picture emerging from previous studies at Campi Flegrei caldera. Although clearly an idealisation, a number of first order characteristics of possible real magmatic systems at Campi Flegrei caldera are accounted for. They include the more chemically evolved, partially degassed nature of magmas emplaced at shallow depths, and the likely occurrence of multiple reservoirs with different depth, size and shape which can be connected at certain stages during system evolution. If that happens, deeper, CO_2-rich magmas may rise and rejuvenate the shallow magmas.

1 The Magmatic System of the Campi Flegrei Caldera

The Campi Flegrei caldera (CFc) is the dominant feature of the Campi Flegrei volcanic field (Chap. Volcanic and Deformation History of the Campi Flegrei Volcanic Field, Italy). It is a complex, nested structure formed by the Campanian Ignimbrite (CI; ~40 ka) and the Neapolitan Yellow Tuff (NYT; ~15 ka) eruptions (Orsi et al. 1992, 1996; Chap. Volcanic and Deformation History of the Campi Flegrei Volcanic Field, Italy). The NYT caldera has been the site of an intense volcanic and deformation activity (Orsi et al. 1996, 1999, 2004; Di Vito et al. 1999; Smith et al. 2011; Chap. Volcanic and Deformation History of the Campi Flegrei Volcanic Field, Italy). Volcanism has generated no less than 70 eruptions, among which Agnano-Monte Spina (4,482–4,625 cal. years BP; de Vita et al. 1999; Arienzo et al. 2010; Smith et al 2011), Minopoli 2

C. P. Montagna (✉) · P. Papale · A. Longo
Istituto Nazionale di Geofisica e Vulcanologia, Sezione di Pisa, Pisa, Italy
e-mail: chiara.montagna@ingv.it

G. Orsi et al. (eds.), *Campi Flegrei*, Active Volcanoes of the World,
https://doi.org/10.1007/978-3-642-37060-1_7

(~11 ka; Di Vito et al. 1999; Di Renzo et al. 2011; Tomlinson et al. 2012) and Fondo Riccio (~11 ka; Di Vito et al. 1999; Di Renzo et al. 2011; Tomlinson et al. 2012).

The magmatic system of the CFc can be reconstructed based on information from various geophysical surveys as well as analyses of eruptive products of past eruptions, as detailed in Chaps. Seismic and Gravity Structure of the Campi Flegrei Caldera, Italy; An Evolutionary Model for the Magmatic System of the Campi Flegrei Volcanic Field (Italy) Constrained by Petrochemical Data; Origin and Differentiation History of the Magmatic System Feeding the Campi Flegrei Volcanic Field (Italy) Constrained by Radiogenic and Stable Isotope Data; Tephrochronology and Geochemistry of Tephra from the Campi Flegrei Volcanic Field, Italy; Rheological Properties of the Magmas Feeding the Campi Flegrei Caldera (Italy) and Their Influence on Mixing Processes. Analyses of seismic records allow us to infer the position and location of fluids within the host rock (Judenherc and Zollo 2004; Zollo et al. 2008; De Siena et al. 2010; Masterlark et al. 2010; Chouet and Matoza 2013). A seismic reflection horizon at around 8 km depth possibly identifies the top of a partially molten region, probably as wide as some tens of kilometres in the horizontal direction, most likely representing a magmatic sill (Judenherc and Zollo 2004; Zollo et al. 2008; Pappalardo and Mastrolorenzo 2012).

A variety of observations suggests that small batches of magma have been forming throughout the caldera history (De Siena et al. 2010; Di Renzo et al. 2011). Crystallised magma bodies, sized less than 1 km^3, have been recognised by processing offshore seismic lines, at depths ranging between less than 1 and 6 km (Piochi et al. 2014). Fluid-rich batches interpreted as partially molten magma have been identified by seismic attenuation tomography in the same depth range (De Siena et al. 2010). Reconstructed phase equilibria for the Agnano-Monte Spina eruption, as well as H_2O and CO_2 contents in melt inclusions from Minopoli 2, Fondo Riccio, and Agnano-Monte Spina confirm that magmas had been residing at all depths less than about 9 km (Roach 2005; Mangiacapra et al. 2008; Arienzo et al. 2010; Piochi et al. 2014; Astbury et al. 2018; Chaps. Volcanic and Deformation History of the Campi Flegrei Volcanic Field, Italy; Seismic and Gravity Structure of the Campi Flegrei Caldera, Italy; An Evolutionary Model for the Magmatic System of the Campi Flegrei Volcanic Field (Italy) Constrained by Petrochemical Data; Origin and Differentiation History of the Magmatic System Feeding the Campi Flegrei Volcanic Field (Italy) Constrained by Radiogenic and Stable Isotope Data). Small, shallow magma bodies have been identified as actively involved in past eruptions, which at least in some cases shortly followed the arrival of volatile-rich, less differentiated magmas from greater depth (Arienzo et al. 2009, 2010; Fourmentraux et al. 2012; Astbury et al. 2018; Chaps. An Evolutionary Model for the Magmatic System of the Campi Flegrei Volcanic Field (Italy) Constrained by Petrochemical Data; Origin and Differentiation History of the Magmatic System Feeding the Campi Flegrei Volcanic Field (Italy) Constrained by Radiogenic and Stable Isotope Data). Preferential pathways for magma ascent have often been related to caldera structures (Akande et al. 2019).

The composition of the erupted products ranges from shoshonitic to trachytic to phonolitic; geochemical analyses on melt inclusions suggest a variety of processes during inter-eruptive periods including magma recharge, intra-chamber mixing, and entrapment of phenocrysts left from previous eruptions (Arienzo et al. 2010; Forni et al. 2018; Chaps. An Evolutionary Model for the Magmatic System of the Campi Flegrei Volcanic Field (Italy) Constrained by Petrochemical Data; Origin and Differentiation History of the Magmatic System Feeding the Campi Flegrei Volcanic Field (Italy) Constrained by Radiogenic and Stable Isotope Data).

From all the above, a schematic picture of the CFc magmatic system can be derived (Fig. 1). It includes the deep magmatic sill containing the poorly evolved, CO_2-rich shoshonitic magma; and more or less persistent features, such as

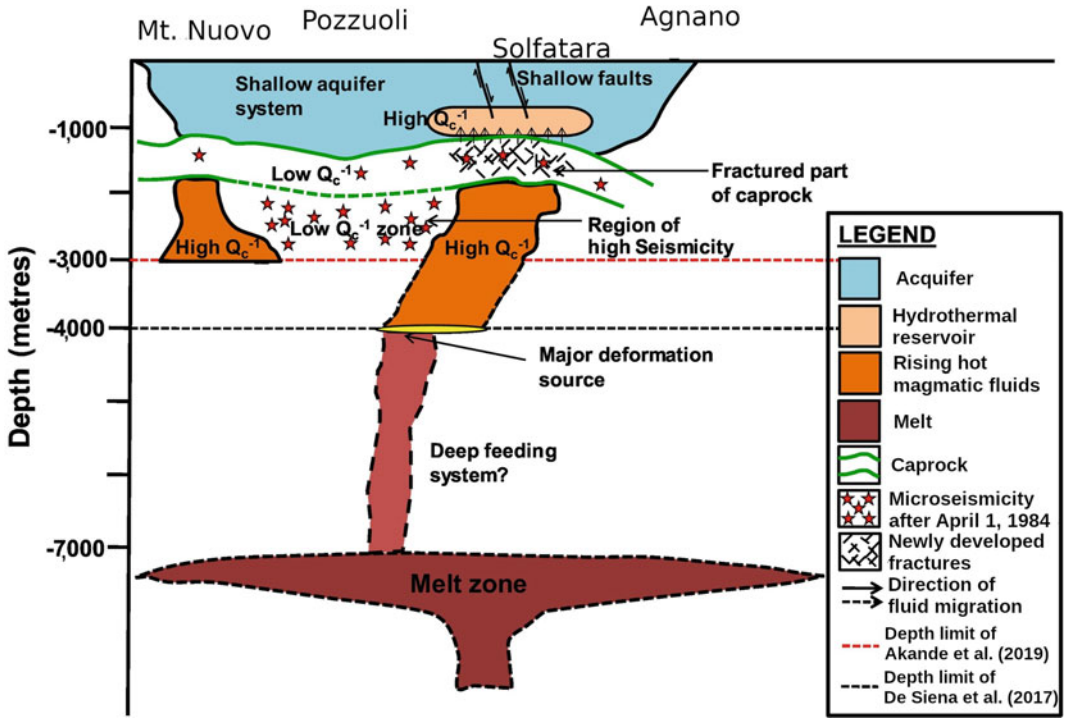

Fig. 1 Scheme of the shallow magmatic system beneath the Campi Flegrei caldera. Figure modified after Akande et al. (2019)

dikes, fractures or conduits, possibly related to caldera structures, linking the deep reservoir to shallower, degassed, more crystal-rich batches of magma. Shallower reservoirs contain magmas with compositions from trachyte to phonolite. Mingling and mixing of shallow magma with others coming from depth is thought to be a recurrent process in the CFc volcanism, often invoked as the main trigger of past eruptions (Arienzo et al. 2011; Fourmentraux et al. 2012; Astbury et al. 2018; Chaps. An Evolutionary Model for the Magmatic System of the Campi Flegrei Volcanic Field (Italy) Constrained by Petrochemical Data; Origin and Differentiation History of the Magmatic System Feeding the Campi Flegrei Volcanic Field (Italy) Constrained by Radiogenic and Stable Isotope Data). Eruptive products preserve the signature of such processes, and provide clues about the time scales of mixing, that in most cases appear to last only hours to days before the eruption (Perugini et al. 2010, 2015a, b; Morgavi et al. 2017; Chap. Rheological Properties of the Magmas Feeding the Campi Flegrei Caldera (Italy) and Their Influence on Mixing Processes). The regional and/or local stress regimes allow the deep magmas to rise to shallow levels, either along established pathways or cracking the host rocs and creating new ones (Orsi et al. 1996, 1999). When the rising magma encounters a molten or partially molten region, the residing magma gets rejuvenated and mixes with the incoming one (Bachmann and Bergantz 2003). At CFc, magmas rising from depth are typically rich in gas, especially CO_2 (Mangiacapra et al. 2008; Arienzo et al. 2010; Moretti et al. 2013). When such magmas reach an already established reservoir where more dense and viscous magma resides, they tend to rise under the action of buoyancy forces. The compositionally different magmas mix first physically, and, on longer time scales, chemically, producing intermediate compositions (Arienzo et al. 2009; Tonarini et al. 2009; Perugini et al. 2010; Di Renzo et al. 2011).

2 Physical Model for the Campi Flegrei Caldera Magmatic System

2.1 Magma Chamber Processes

Magma chamber dynamics is governed by a variety of microscopic and macroscopic physical and chemical processes, which range from periodic magma injections, to mixing and mingling of different magmas, to magma differentiation due to crystal fractionation and melt segregation, to heat and mass transfer between the phases and with the surrounding rocks, to interaction with the host rock and its tectonic stresses (Sigurdsson et al. 2015). The quantitative study of magma dynamics is complicated by the uncertainties about the characteristics of the magmatic system, which is out of direct observation. Nevertheless, all of the aforementioned processes bear consequences on the state of the reservoir, which can be inferred by analysing either the petrological records (e.g., Perugini and Poli 2012) or the geophysical signals indicating movement at depth (e.g., Bagagli et al. 2017).

A precise understanding of the physics of magmatic reservoirs is still lacking (Cashman et al. 2017). Magma is a multi-phase, multi-component fluid and as it rises and stalls in the Earth's crust it encounters very different pressure and temperature conditions, as well as stress and strain, that determine the phase assemblage and its evolution in space and time. The thermodynamics and fluid dynamics of such a mixture are quite complex as they involve phase changes between melt, gas and crystals, which in turn contribute to determine the physical and rheological properties governing its motion (Bachmann and Bergantz 2006; Degruyter and Huber 2014; Parmigiani et al. 2014; Bergantz et al. 2015; Montagna et al. 2015; Papale et al. 2017).

It is more and more commonly being assumed that the typical magmatic reservoir comprises a highly crystalline mushy region, and possibly a smaller, melt-rich portion at its top (Schleicher and Bergantz 2017; Cashman et al. 2017). Long-lived magma chambers can slowly solidify and originate mush zones that are dominated by crystals (Pistone et al. 2017). The relative importance of the mushy with respect to the melt-dominated regions in determining the evolution of the system is hard to assess, as is the relative volume and mass ratios of the two. Models that describe magma chamber dynamics have either focussed on one or the other of the two regimes (Bachmann and Bergantz 2006; Montagna et al. 2015; Papale et al. 2017); moreover, to model the mushy region different approaches have been used, from fluid-like to porous flow, to brittle fracturing (Parmigiani et al. 2014; Carrara et al. 2019).

Convection, mingling and mixing are among the most common processes in melt-dominated as well as mushy reservoirs (Schleicher and Bergantz 2017; Morgavi et al. 2017), but their features can significantly differ among the two (Parmigiani et al. 2014; Montagna et al. 2015). Mingling refers to mechanical mixing of two or more batches of magma, without chemical exchanges between them; on the contrary, mixing involves chemical exchanges whereby elements diffuse according to compositional gradients (e.g., Flinders and Clemens 1996).

One of the first numerical models for mixing of incompressible homogeneous magmas due to diffusion and thermal-compositional convection was developed by Oldenburg et al. (1989, and references therein). Diffusive convection can be originated by both thermal and compositional gradients, that give rise to a boundary layer instability developing on time scales that, for typical magmatic systems, are on the order of years to thousands of years, depending mostly on the viscosities of the magmas involved (Spera et al. 1982).

On the other hand, mingling in melt-dominated reservoirs (e.g., Andersen et al. 2019; Gualda et al. 2019) can be originated by Rayleigh–Taylor instability as a volatile-rich magma reaches a degassed reservoir (Ruprecht et al. 2008). This process can happen on much shorter time scales, on the order of hours to days (Montagna et al. 2015). Over such short time spans, the interacting magmas are effectively immiscible, and chemical diffusion is negligible,

albeit a limited amount of numerical diffusion is inevitably present (Longo et al. 2012a).

2.2 Models of Magma Dynamics

The physical model in Longo et al. (2012a) describes the time-dependent dynamics of a multicomponent mixture consisting of liquid (or crystal suspension) in thermodynamic equilibrium with an $H_2O + CO_2$ gas phase at the local conditions of pressure, temperature and composition. The model can handle both compressible and incompressible flows, therefore it is particularly apt to solve for magmatic mixtures characterised by a very low compressibility at depth, where most volatiles are dissolved in the melt, that increases at shallower depths as volatiles begin to exsolve. The numerical algorithm used in the solution of the conservation equations is based on an extension of the finite element formulation by Hauke and Hughes (1998) to include multicomponent fluids (Longo et al. 2006), allowing the investigation of processes involving mixing of fluids, chemical changes, and phase transitions. The algorithm consists of a space–time discretisation with Galerkin least-squares and discontinuity capturing terms, with third order accuracy in time and space. This method allows the simulation of both compressible and incompressible flow dynamics (Shakib et al. 1991; Chalot and Hughes 1994; Hauke and Hughes 1998), and it is effective in stabilising the numerical solution without introducing excessive numerical diffusion. A large number of problems can be solved, such as natural and forced convection, shock waves and their interaction with contact discontinuities, evolution of internal interfaces in incompressible or compressible flows, and bubbly flows with evaporation or gas dissolution. All of these processes are relevant for magmatic systems, and the model has been successfully applied to obtain significant results on magma reservoir dynamics in different magmatic settings including basaltic, andesitic and dacitic systems (Longo et al. 2012b; Montagna et al. 2015; Papale et al. 2017; Garg et al. 2019). The conservation equations for the mass of single components and momentum of the whole mixture, together with the gas–liquid thermodynamic equilibrium model and the constitutive equations for mixture properties (density and viscosity), are discretised and solved for the primitive variables pressure, velocity, temperature, and concentration of components. Magmas are described as ideal mixtures with components that may be either in the liquid or gaseous state, with instantaneous phase change according to the non-ideal multicomponent $H_2O + CO_2$ saturation model of Papale et al. (2006). Gas bubbles are assumed to be non-deformable, a good approximation if the bubble size is smaller than ~ 10 m (Marchetti et al. 2004). This corresponds to a gas volume of 5–50% for bubble number densities in the range 10^{14} to 10^{15} m^{-3}. Such small bubble sizes justify the gas–melt coupled flow assumption, as well as the equilibrium thermodynamics (Burgisser et al. 2005; Yoshimura and Nakamura 2011). The role on the relevant properties (density and viscosity) of dissolved water and of the dispersed gas and solid phases, and the mutual roles of H_2O and CO_2 in affecting their saturation contents, are accounted for. Mixture density is calculated using the Lange (1994) equation of state for the liquid phase, real gas properties and standard mixture laws for multiphase fluids. Mixture viscosity (under the assumption of Newtonian rheology) is computed through standard rules of mixing (Reid et al. 1977) for one-phase mixtures and with a semi-empirical relation (Ishii and Zuber 1979) in order to account for the effect of non-deformable gas bubbles. Liquid viscosity is modelled as in Giordano et al. (2008), and it depends on liquid composition and dissolved water content.

The solid phase (suspended crystals) can be taken into account in the computation of mixture properties (density and viscosity). Nevertheless, in the models shown here the magmas are assumed crystal-free as most erupted products with the compositions used have been found to have very little phenocrysts (Mangiacapra et al. 2008). The model is meaningful for melt-dominated, crystal-poor magma reservoirs, which is expected to be the case for many eruptions at Campi Flegrei (Di Renzo et al. 2011;

Forni et al. 2018; Chaps. An Evolutionary Model for the Magmatic System of the Campi Flegrei Volcanic Field (Italy) Constrained by Petrochemical Data; Origin and Differentiation History of the Magmatic System Feeding the Campi Flegrei Volcanic Field (Italy) Constrained by Radiogenic and Stable Isotope Data). A crystal-rich, mushy region is also hypothesised to have been involved in the CI eruption (Forni et al. 2018); this work focuses on smaller eruptions that have not been energetic enough to tap the crystal-rich regions of the reservoirs.

The magmatic system of CFc is approximated as isothermal: temperature differences inferred from melt inclusion data are negligible (Mangiacapra et al. 2008), and solving the dynamics for an isothermal system greatly reduces computational needs as the energy conservation equation does not need to be solved. The effects of wall cooling can be neglected on the very short time scales analysed here (Sect. 4).

2.3 Modelling the Magmatic System of the Campi Flegrei Caldera

In order to understand the dynamics of magmas beneath the CFc, the magmatic system is simplified to retain its most essential features. The specific aim is to explore the mixing process, and the dependence of its efficiency and time scales on the simulation conditions. Other details on the time scales, the evolution of pressure in the different portions of the magmatic system as well as the ground deformation signals related to the dynamics described here are analysed in separate studies (Montagna et al. 2015, 2017; Bagagli et al. 2017; Morgavi et al. 2017; Papale et al. 2017).

The model describes the injection of CO_2-rich, shoshonitic magma coming from a deep reservoir into a shallower, much smaller chamber, containing more evolved and partially degassed phonolitic magma. The deep reservoir is schematised as a sill; the geometry of the shallow chamber has been varied from oblate to prolate in a set of simulations, as shown in Fig. 2. Initial conditions for the simulated cases are reported in Table 1.

The top of the deep reservoir is at 8 km depth, and its horizontal and vertical semi-axes measure 4 km and 0.5 km, respectively. The shallow reservoir has its top at 3 km depth below the surface; its surface area is kept to 0.25×10^6 m^2, representing a volume of magma in the order of a few tenths of km^3 (Chaps. Volcanic and Deformation History of the Campi Flegrei Volcanic Field, Italy; Seismic and Gravity Structure of the Campi Flegrei Caldera, Italy; An Evolutionary Model for the Magmatic System of the Campi Flegrei Volcanic Field (Italy) Constrained by Petrochemical Data; Origin and Differentiation History of the Magmatic System Feeding the Campi Flegrei Volcanic Field (Italy) Constrained by Radiogenic and Stable Isotope Data; Source Modelling from Ground Deformation and Gravity Changes at the Campi Flegrei Caldera, Italy). The oxides composition of the two magmas is detailed in Table 2.

At the initial time, the two magmas are placed in contact at the bottom of the shallow chamber (top of the feeding dyke; Fig. 2). Because of the higher volatile content, thus lower overall density of the deeper magma, the system is gravitationally unstable. Therefore, the deep magma tends to rise into the shallow chamber, pushing the resident magma down through the feeding dike.

The initial condition aims at reproducing the effects of chemical processes such as compositional evolution and degassing, which contribute to a density increase in the shallow regions of a spatially extended, interconnected magmatic system (e.g., Kazahaya et al. 1994), possibly through permanently open pathways (e.g., Di Renzo et al. 2011). As such a system is expected to be in continuous evolution, any choice of initial conditions would be equally arbitrary, therefore the extreme case is explored here, where buoyancy forces are most effective and acting at shallow chamber inlet. Analysis of results focuses on the long-term dynamics, neglecting the transient dictated by the choice of initial conditions.

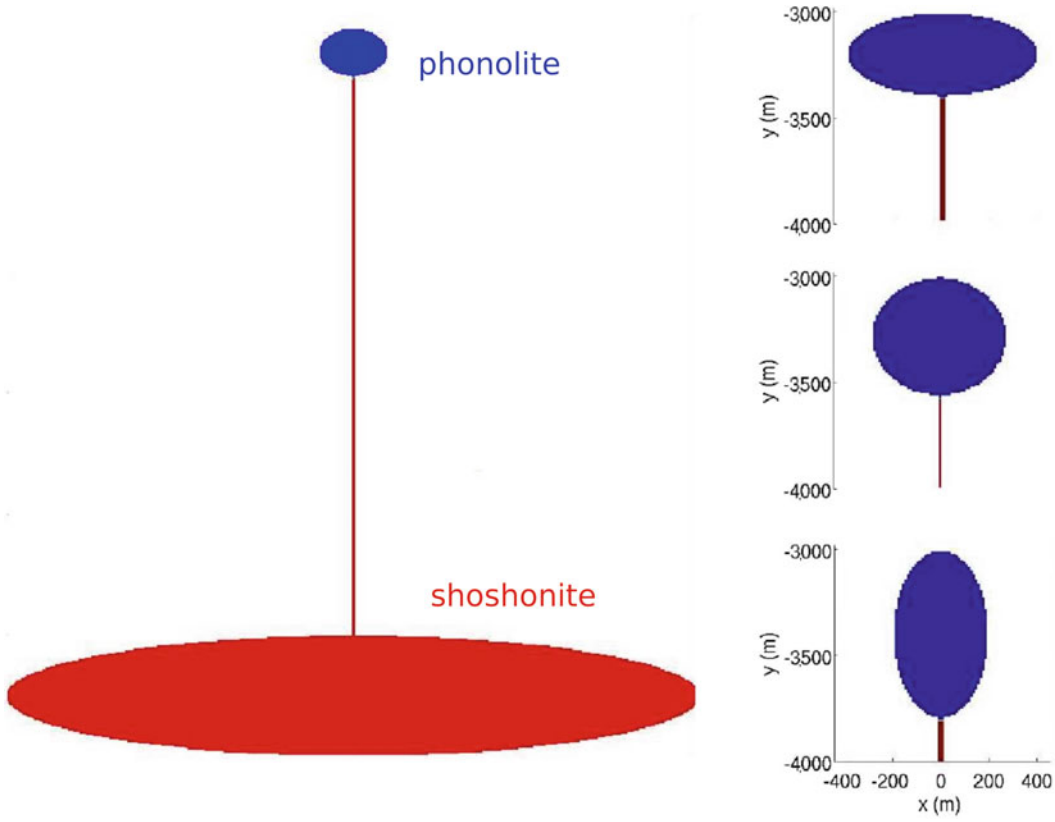

Fig. 2 The whole simulated system alongside the three different geometrical settings for the shallower magma chamber at the Campi Flegrei caldera. Top: horizontally elongated, sill-like chamber. Centre: Circular chamber. Bottom: vertically elongated, dike-like chamber. Figure modified after Montagna et al. (2017)

Table 1 List of simulations and their initial conditions

Simulation No.		1	2	3	4	5
Assumed initial conditions	CO_2 shoshonite (wt%)	1	1	1	1	1
	CO_2 phonolite (wt%)	0.3	0.3	0.3	0.3	0.3
	H_2O shoshonite (wt%)	2	2	2	2	2
	H_2O phonolite (wt%)	2.5	2.5	2.5	1	1
	Geometry of shallow chamber	Oblate	Prolate	Circular	Oblate	Prolate
Calculated initial conditions	Density contrast at initial interface (kg/m^3)	30	20	20	20	140
	Gas volume at initial interface, shoshonite (vol%)	10	8	9	9	8
	Gas volume at initial interface, phonolite (vol%)	5	4	5	2	2
	Gas volume at system top (vol%)	7	7	7	2	2
	Gas volume at system bottom (vol %)	3	3	3	3	3

Data from Montagna et al. (2015), Bagagli et al. (2017), Papale et al. (2017)

Table 2 Oxides contents (unit fraction) for the two end-member magmas, shoshonite (Sho) and phonolite (Pho)

	SiO_2	TiO_2	Al_2O_3	Fe_2O_3	FeO	MnO	MgO	CaO	Na_2O	K_2O
Sho	0.48	0.012	0.16	0.021	0.063	0.0014	0.10	0.12	0.028	0.015
Pho	0.54	0.0060	0.20	0.016	0.032	0.0014	0.017	0.068	0.047	0.079

Data from Montagna et al. (2015)

Different setups have been explored in order to highlight the roles played by the geometry of the magmatic system and by the extent of previous degassing of the shallow magma. Keeping the upper chamber top at a depth of 3 km and its 2D cross-sectional area constant, its geometry was varied from a sill to a circle and to a vertically elongated, dike-like ellipsoid. For the two ellipsoidal chambers, the volatile content of the shallow phonolitic magma was also reduced to 1 wt% H_2O and 0.1 wt% CO_2, compared to 2.5 wt % H_2O and 0.3 wt% CO_2 of the previous set of simulations. The deep shoshonitic magma contains in all cases 2 wt% H_2O and 1 wt% CO_2 (Table 1; Chaps. An Evolutionary Model for the Magmatic System of the Campi Flegrei Volcanic Field (Italy) Constrained by Petrochemical Data; Origin and Differentiation History of the Magmatic System Feeding the Campi Flegrei Volcanic Field (Italy) Constrained by Radiogenic and Stable Isotope Data). It is worth noting that such quantities are total volatile amounts, and they are distributed between liquid and gas phases according to the local conditions and the saturation model of Papale et al. (2006). The simulated systems are closed, with fixed boundaries. The effect of wall-rock elasticity on the chamber dynamics is neglected, as it is assumed to cause small pressure changes with respect to those originating from the magma dynamics.

The system setup is two-dimensional mainly to keep computational efforts affordable. Extension to full 3D systems should not bring about any substantial difference in the convective patterns observed: the third dimension would give rise to different dominant modes of the Rayleigh–Taylor instability (Ribe 1998), thus possibly modifying (either increasing or decreasing, depending on the amplitude of the initial perturbation) the efficiency of transport, but not substantially (Kaus and Podladchikov 2001).

The setups shown here are based on petrological and geophysical evidence, as detailed in Sect. 1; a more rigorous exploration of parameters' space is at the moment limited by computational resources. Nevertheless, the results are meaningful for a class of processes that have been hypothesised to be relatively common at CFc (e.g., Troise et al. 2019).

3 Dynamics of Magma Reservoir Processes at the Campi Flegrei Caldera

The simulations reveal detailed patterns of magma convection and mixing taking place in the upper chamber + feeding dyke domains. In order to illustrate those patterns, a reference simulation (corresponding to simulation no. 4 in Table 1) is chosen, and the other cases are described through comparison with the reference one.

The reference simulation takes into account a situation where the shallow chamber had previously degassed efficiently. Consequently, the density contrast between the two magma types at the initial magma interface is relatively large, corresponding to about 120 kg/m^3. The shallow reservoir is horizontally elongated.

Figure 3 summarises the results in terms of the relevant quantities—composition, density and gas volume fraction—that are shown at four different times up to 5 h of real time. The dynamics is triggered by a Rayleigh–Taylor instability, as the resident phonolitic magma has a higher density that the shoshonite. The development of the instability and its time scales are independent of the volumes of intruding magmas

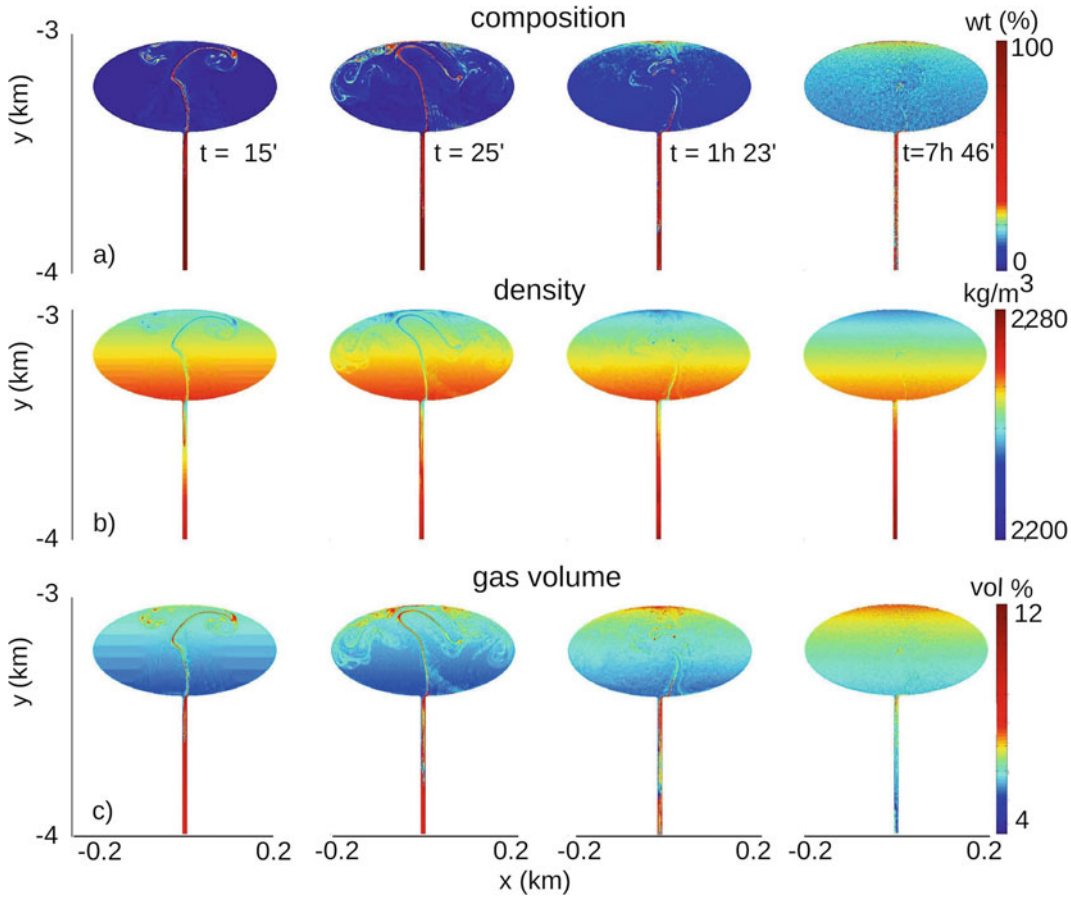

Fig. 3 Snapshots of composition, density and gas volume fractions at different simulated times in the shallower part of the system. Figure modified after Papale et al. (2017)

(e.g., Bellman and Pennington 1954; Seropian et al. 2018).

Soon after the start of the simulation, disruption of the initial interface by buoyancy forces produces a series of discrete plumes of light magma rising through the shallow chamber and reaching its top after having developed complex velocity fields. At the same time, part of the dense magma originally hosted in the shallow chamber sinks into the feeding dyke. Intense mixing originates at the dyke level, so that no pure shoshonitic end-member can be found in the shallow chamber; the rising plumes are rather made of a mixture with 30 to 50 wt% deep component. In this framework, only mechanical mixing is considered, as chemical reactions apart from volatile exsolution/dissolution are not implemented in the numerical scheme. Therefore, mixing at the scale of the simulation, with maximum resolution in the order of 1 m, refers to mechanical mingling rather than chemical mixing. The simulated dynamics suggests a complex pattern of convection and mixing (or mingling) whereby the original dense magma mixes with the volatile-rich, lighter magma coming from depth at chamber bottom or dyke level. The original phonolite carried down into the dyke mixes with the shoshonite; the mixed magma is overall lighter than the magma above it or in its immediate surroundings, therefore part of the initially sunk magma is carried up again into the shallow chamber, while other portions continue to sink down into the dyke. This complex process originates a compositional, density, and gas

volume stratification inside the chamber, with maximum gas volumes at chamber top of about 6 vol%. In the meantime, the original density contrast at chamber bottom is disrupted and a smoother and smoother density profile is created, so that the convective process tends to slow down in time. Figure 4 shows the time distribution of the efficiency of convection η_C for all performed simulations, defined as the variation in time of phonolite mass in the shallow chamber, normalised to the initial amount so to allow direct comparison of the different cases:

$$\eta\eta_C = \frac{|m_R(t) - m_R(0)|}{m_R(0)} \quad (1)$$

In the above, m_R(t) is the mass of the initially resident phonolitic magma as a function of time.

A number of relevant aspects of the simulated dynamics must be highlighted. First of all, in all cases the total mass in the shallow chamber decreases with time as a consequence of average density decrease, due to the partial substitution of the initial dense phonolite with the lighter gas-rich shoshonite. In the most efficient case, corresponding to the reference case described above, the total mass in the shallow chamber has decreased by less than 2 wt% after about 5 h of convection and mixing. Second, the efficiency of convection increases substantially with the extent of degassing of the magma initially residing in the chamber (cases 1, 2 and 3 correspond to lower degassing extent, see Table 1; Fig. 4). Third, convection and mixing tend to slow down with time, as revealed by the progressive decrease of the slopes in Fig. 4. More than 80% of the dense, degassed magma initially residing in the chamber remains at chamber level after waning of the convective process (as in case 1, where an asymptotic trend clearly emerges). Thus, the complex patterns of convection and mixing described above are such that most of the degassed magma is not carried down to larger depths when a new stable profile has been created. While shallow chamber degassing creates unstable conditions by increasing the density of the magma at shallow levels, the ingression of small amounts of volatile-rich magma rapidly re-establishes a new "equilibrium". The new overall stability is a dynamic condition: even at the

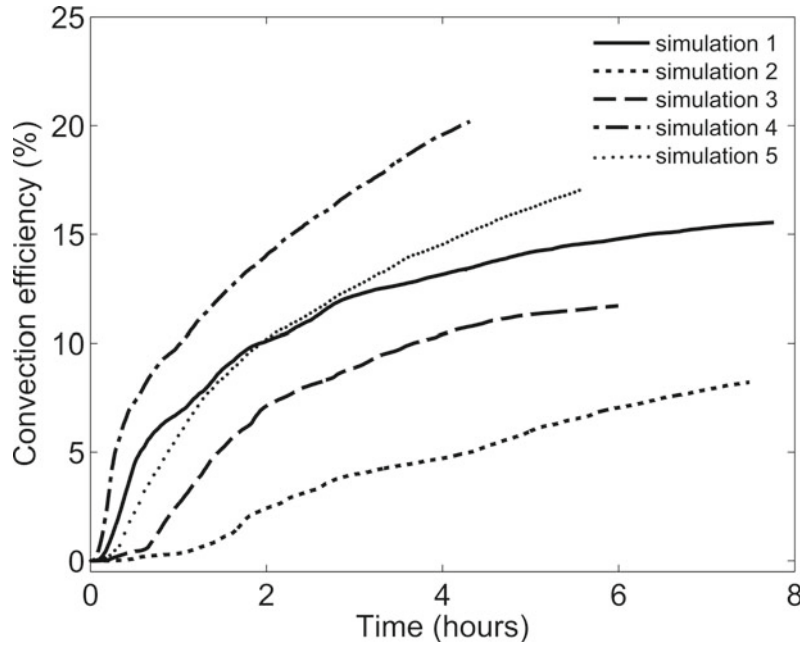

Fig. 4 Convection efficiency in the shallow reservoir for the different simulations as function of time. The simulation number is the same as in Table 1. Figure modified after Montagna et al. (2015)

longest simulated times, small batches of mixed magma still enter the chamber while other batches sink into the dyke, overall keeping a more or less constant balance of total mass and of single magmatic components in the chamber. The overall dynamics is not expected to drastically change after some hours, as in the simulated conditions the gravitational instability that triggers magma interaction is obliterated by the dynamics itself, as the density profile becomes more and more stable. On geological time scales, this time span seems irrelevant; nevertheless, petrological analyses on erupted products at CFc retrieve similar time scales for efficient mingling to take place (Perugini et al. 2010, 2015a, b; Chap. Rheological Properties of the Magmas Feeding the Campi Flegrei Caldera (Italy) and Their Influence on Mixing Processes). The results shown here provide a means for interpreting those data in relation to dynamical processes at depth.

Finally, the trends in Fig. 4 show that the efficiency of convection depends on the shallow chamber geometry in such a way that it decreases when its horizontal dimension also decreases. This is expected, as the efficiency of natural convection depends on the system dimension perpendicular to the driving force represented by gravity. That is also visible from the colour plots in Fig. 5, which show a progressive deeper blue (that is, lower proportion of deep magmatic component) when moving from oblate to circular to prolate chamber geometry. At the same time, however, the more prolate geometries result in more pronounced accumulation of volatile-rich deep component at the chamber top, thus more pronounced chamber stratification.

It is also noteworthy that the plumes of lighter magma tend to rise through the chamber following significantly different patterns. Rising plumes tend to follow the chamber walls for much longer distances in prolate geometries,

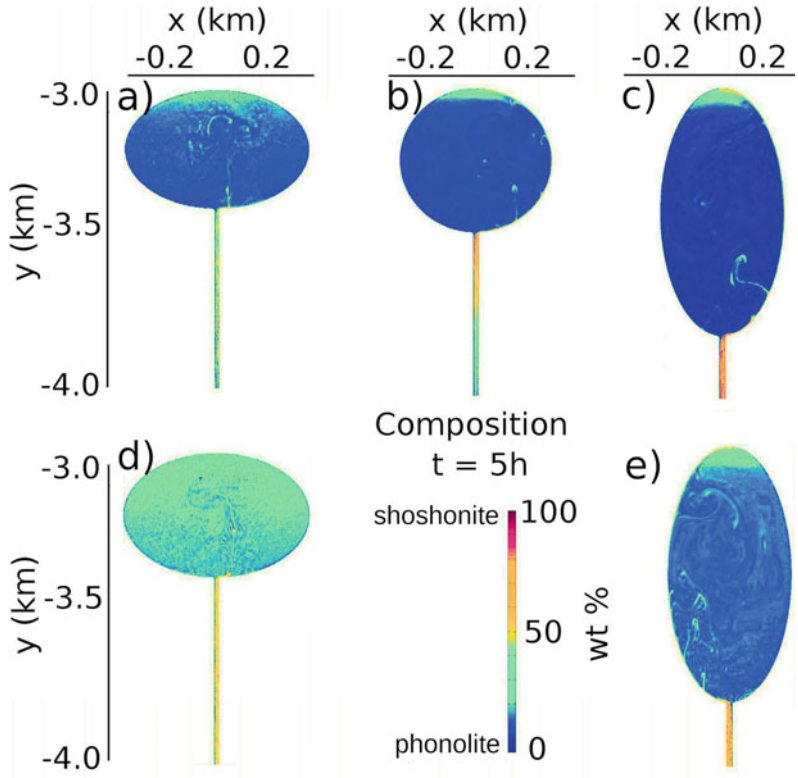

Fig. 5 Composition in the upper chamber after 5 h of simulated time. From left to right, top to bottom, order of simulations as in Table 1: **a** simulation 1, low density contrast, horizontal chamber; **b** simulation 2, low density contrast, circular chamber; **c** simulation 3, low density contrast, vertical chamber; **d** simulation 4, reference simulation, high density contrast, horizontal chamber; **e** simulation 5, high density contrast, vertical chamber. Figure modified after Montagna et al. (2015, 2017)

generating roughly one single convective cell in the chamber. This optimizes convection, thus partly balancing the effects of decreased horizontal chamber size diminishing the extent to which the convection efficiency is reduced when moving from oblate to prolate geometries.

4 Multi-disciplinary Interpretation of Modelling Results

This study focuses on the convection and mixing dynamics occurring in a shallow chamber when it is intersected by a dyke carrying more primitive, volatile-rich (especially CO_2) magma from a deeper reservoir. The system conditions refer to a general situation appropriate for the volcanism of the CFc, dominated by the emplacement of relatively small magma chambers at shallow levels, repeatedly recharged by deeper magma while undergoing shallow system degassing (Aiuppa et al. 2013; Di Renzo et al. 2016; Chaps. Volcanic and Deformation History of the Campi Flegrei Volcanic Field, Italy; Seismic and Gravity Structure of the Campi Flegrei Caldera, Italy; An Evolutionary Model for the Magmatic System of the Campi Flegrei Volcanic Field (Italy) Constrained by Petrochemical Data; Origin and Differentiation History of the Magmatic System Feeding the Campi Flegrei Volcanic Field (Italy) Constrained by Radiogenic and Stable Isotope Data). The volcanic products reveal magma mixing mostly from melt-crystal (Roach 2005) and isotopic (Arienzo et al. 2009, and references therein; Chap. Origin and Differentiation History of the Magmatic System Feeding the Campi Flegrei Volcanic Field (Italy) Constrained by Radiogenic and Stable Isotope Data) disequilibrium, as well as from melt inclusions within crystals (Arienzo et al. 2010). While mixing between different magmas is a widespread occurrence at the CFc, magmatic end-member components are usually not identified at the macroscopic scale in the volcanic products, especially for the deeper, less chemically evolved components the presence of which emerges only from detailed chemical and petrographic analyses (Astbury et al. 2018). On the other hand, time scales of magma mixing can be quite short, of the order of hours to days, as it is revealed by both time-scales of melt-crystal disequilibrium (Roach 2005) and by the application of a diffusive fractionation model of trace elements to a number of relevant eruptions in the CFc history (De Campos et al. 2008; Perugini et al. 2010, 2015a, b; Chap. Rheological Properties of the Magmas Feeding the Campi Flegrei Caldera (Italy) and Their Influence on Mixing Processes).

Although a full comparison is limited by the resolution of the computational grid, which is on the order of 1 m, the present numerical simulations provide a fully consistent picture: in all simulated cases, the deep, less evolved, volatile-rich end-member magma involved in the mixing process is rapidly lost as an individual component, while magma mixing results in a stratified but substantially laterally homogeneous (at the resolved spatial scale) composition on a short time-scale of a few to 10 h. In addition, the simulations suggest a relevant role of magma mixing at the feeding dyke level, and highlight complex patterns whereby the partially degassed magma originally hosted at shallow levels can sink down into the dyke, mix with the rising volatile-rich magma, then re-enter into the chamber as a mixture component masking the end-member characteristics of the deep rejuvenating magma. The evolution of pressure within the system is highly heterogeneous in space and time, as detailed in Papale et al. (2017). Calculated pressure variations are always smaller than 1 MPa, therefore large variations of the system volume, especially in the dyke, are not expected as a consequence of the exchange dynamics described above. Nevertheless, detectable ground deformation and seismicity can be generated by the convective dynamics, characterised by specific frequency patterns that could potentially be used to infer magma movement at depth from the monitoring records (Longo et al. 2012b; Bagagli et al. 2017; Chaps The Permanent Monitoring System of the Campi Flegrei Caldera, Italy; Source Modelling from Ground Deformation and Gravity Changes at the Campi Flegrei Caldera, Italy).

The numerical simulations shown here (see also Montagna et al. 2015, 2017; Papale et al.

2017) are limited by the huge computational time they require, therefore, only some hours of real time have been explored till now. A conceptual extrapolation to much longer times is allowed by the fact that in some of the simulated cases, and specifically in case 1 corresponding to the longest simulated time (about 8 h), a condition is reached where the initial gravitational instability is completely destroyed and new dynamically stable conditions are established. Thus, the simulation describes an entire mixing cycle in which the initial density contrast is totally removed, and a new dynamic equilibrium is reached. All other simulations show the same tendency, as it is suggested by the progressive flattening of the convection efficiency curves in Fig. 4, although over the simulated times a stable condition is in most cases approached but not reached. The trigger for the whole process is provided by the fact that the shallow magma is initially partially degassed, therefore its density is, at same pressure conditions, larger than the density of the magma rising from depth. This is the origin of the gravitational instability in the initial conditions.

Magmatic bodies emplaced at shallow level are known to degas efficiently, as a consequence of relatively large gas volumes at low pressure conditions and brittle rock mechanics allowing the generation of cracks providing pathways for gas escape towards the surface. In the specific case of the CFc, an abundant magmatic gas component is recognised in the fumaroles of La Solfatara crater (Caliro et al. 2007; Chiodini et al. 2015; Tamburello et al. 2019; Chaps. The Permanent Monitoring System of the Campi Flegrei Caldera, Italy; The Hydrothermal System of the Campi Flegrei Caldera, Italy), that globally discharge about 1,500 tons/day of CO_2 in the atmosphere (Caliro et al. 2007). The final condition in all simulations is the establishment of a gas-rich cap at the top of the shallow chamber (Figs. 3 and 5). It is expected that over a longer time this would feed a new efficient degassing phase, as gas-rich magma continues to slowly accumulate at the top of the system to then seep through the chamber roof and propagate through the porous host rock, over much longer time scales than those simulated here (Jasim et al. 2015). Large oscillations in the CO_2 content of the fumarolic gases at La Solfatara are well known (Chiodini et al. 1996, 2015), and more recently, similar oscillations have been proposed to occur in their magmatic component (Moretti et al. 2013). These oscillations follow the major seismic and deformation crisis at CFc in 1982–1984, and they are possibly related to the emplacement of a small magmatic body at 3–4 km depth as revealed by recent seismic attenuation tomography (De Siena et al. 2010; Akande et al. 2019; Chap. Seismic and Gravity Structure of the Campi Flegrei Caldera, Italy), although CO_2 flux can be independent of magmatic flux as it exsolves at large depths (Mangiacapra et al. 2008).

An overall picture emerges: after the emplacement of a small magma body at shallow depth, open system degassing feeding the fumarolic gases (and possibly, partial crystallisation of magma) increases magma density and triggers the arrival of new gas-rich, light magma batches from a deep reservoir, likely along the same pathways that brought the magma to a shallow level. This in turn gives rise to magma convection and mixing, that re-establishes dynamically stable conditions over a short timescale of hours to a few days (increasing with the extent of shallow system degassing). New gas-rich, CO_2-rich magma is accumulated at the top of the shallow chamber, and over a longer time scale of months to years, open system degassing (and crystallisation) increases again the density in the upper system, triggering a new episode of magma injection and repeating the process. Such a sequence can be repeated several times, each time rejuvenating the shallow magmatic system through the injection of small batches of volatile-rich magma from larger depths, and providing new gas that will slowly escape from the system and feed the fumarolic system.

5 Conclusive Remarks

The present numerical simulations are consistent with a number of observations of the CFc volcanism (and to an extent, of several other volcanic products worldwide), although by no

means they are able to describe in detail all of the processes within a deep, complex magmatic system. Such observations include (i) the chemical oscillations observed in the fumarolic gases, that appear to punctuate long-term degassing patterns (Chiodini et al. 2015; Chap. The Hydrothermal System of the Campi Flegrei Caldera, Italy); (ii) the chemical zoning in crystals, that marks oscillations in the P-T-X conditions at crystallisation levels (Astbury et al. 2018; Chaps. An Evolutionary Model for the Magmatic System of the Campi Flegrei Volcanic Field (Italy) Constrained by Petrochemical Data; Origin and Differentiation History of the Magmatic System Feeding the Campi Flegrei Volcanic Field (Italy) Constrained by Radiogenic and Stable Isotope Data); (iii) the presence of melt inclusions in crystals that are in chemical disequilibrium with their host (Tonarini et al. 2009; Chaps. An Evolutionary Model for the Magmatic System of the Campi Flegrei Volcanic Field (Italy) Constrained by Petrochemical Data; Origin and Differentiation History of the Magmatic System Feeding the Campi Flegrei Volcanic Field (Italy) Constrained by Radiogenic and Stable Isotope Data); (iv) the dispersion of volatile contents in melt inclusions that hardly mark simple closed or open system degassing patterns, rather they suggest a widespread occurrence of convection and mixing (a well-studied example is reported for Kīlauea in Barsanti et al. 2009; the melt inclusion data for the Agnano-Monte Spina eruption at the CFc by Arienzo et al. 2010 show similar patterns); (v) the tendency towards rapid homogenisation of magmas upon mixing, preventing macroscopic identification of end-member components (Astbury et al. 2018; Forni et al. 2018; Chaps. An Evolutionary Model for the Magmatic System of the Campi Flegrei Volcanic Field (Italy) Constrained by Petrochemical Data; Origin and Differentiation History of the Magmatic System Feeding the Campi Flegrei Volcanic Field (Italy) Constrained by Radiogenic and Stable Isotope Data; Rheological Properties of the Magmas Feeding the Campi Flegrei Caldera (Italy) and Their Influence on Mixing Processes); (vi) the time-scales of magma mixing as revealed by separate approaches like melt-crystal disequilibrium and trace element diffusive fractionation modelling (Tonarini et al. 2009; Perugini et al. 2015a, b; Chaps. An Evolutionary Model for the Magmatic System of the Campi Flegrei Volcanic Field (Italy) Constrained by Petrochemical Data; Origin and Differentiation History of the Magmatic System Feeding the Campi Flegrei Volcanic Field (Italy) Constrained by Radiogenic and Stable Isotope Data; Rheological Properties of the Magmas Feeding the Campi Flegrei Caldera (Italy) and Their Influence on Mixing Processes).

References

Aiuppa A, Tamburello G, Di Napoli R, Cardellini C, Chiodini G, Giudice G, Grassa F, Pedone M (2013) First observations of the fumarolic gas output from a restless caldera: implications for the current period of unrest (2005–2013) at Campi Flegrei. Geochem Geophys Geosys 14:4153–4169

Akande WG, De Siena L, Gan Q (2019) Three-dimensional kernel-based coda attenuation imaging of caldera structures controlling the 1982–84 Campi Flegrei unrest. J Volcanol Geotherm Res 38:273–283

Andersen NL, Singer BS, Coble MA (2019) Repeated rhyolite eruption from heterogeneous hot zones embedded within a cool, shallow magma reservoir. J Geophys Res-Sol Ea 124:2582–2600

Arienzo I, Civetta L, Heumann A, Horner GW, Orsi G (2009) Isotopic evidence for open system processes within the Campanian Ignimbrite (Campi Flegrei, Italy) magma chamber. Bull Volcanol 71:285–300. https://doi.org/10.1007/s00445-008-0223-0

Arienzo I, Moretti R, Civetta L, Orsi G, Papale P (2010) The feeding system of Agnano Monte Spina eruption (Campi Flegrei, Italy): dragging the past into present activity and future scenarios. Chem Geol 270:135–147

Arienzo I, Heumann A, Horner GW, Civetta L, Orsi G (2011) Processes and timescales of magma evolution prior to the Campanian Ignimbrite eruption (Campi Flegrei, Italy). Earth Planet Sci Lett 306:217–228

Astbury RL, Petrelli M, Ubide T, Stock MJ, Arienzo I, D'Antonio M, Perugini D (2018) Tracking plumbing system dynamics at the Campi Flegrei caldera, Italy: high-resolution trace element mapping of the Astroni crystal cargo. Lithos 318–319:464–477

Bachmann O, Bergantz GW (2003) Rejuvenation of the Fish Canyon magma body: a window into the evolution of large-volume silicic magma systems. Geology 31:789–792

Bachmann O, Bergantz GW (2006) Gas percolation in upper-crustal silicic crystal mushes as a mechanism

for upward heat advection and rejuvenation of near-solidus magma bodies. J Volcanol Geotherm Res 149:85–102

Bagagli M, Montagna CP, Papale P, Longo A (2017) Signature of magmatic processes in strainmeter records at Campi Flegrei (Italy). Geophys Res Lett 44:718–725

Barsanti M, Papale P, Barbato D, Moretti R, Boschi E, Hauri EH, Longo A (2009) Heterogeneous large total CO_2 abundance in the shallow magmatic system of Kilauea volcano, Hawaii. J Geophys Res 144:B12201

Bellman R, Pennington RH (1954) Effects of surface tension and viscosity on Taylor instability. Q Appl Math 12:151–162

Bergantz GW, Schleicher JM, Burgisser A (2015) Open-system dynamics and mixing in magma mushes. Nat Geosci 8:793–796

Burgisser A, Bergantz GW, Breidenthal RE (2005) Addressing complexity in laboratory experiments: the scaling of dilute multiphase flows in magmatic systems. J Volcanol Geotherm Res 141:245–265

Caliro S, Chiodini G, Moretti R, Avino R, Granieri D, Russo M, Fiebig J (2007) The origin of the fumaroles of La Solfatara (Campi Flegrei, South Italy). Geochim Cosmochim Acta 71:3040–3055

Carrara A, Burgisser A, Bergantz GW (2019) Lubrication effects on magmatic mush dynamics. J Volcanol Geotherm Res 380:19–30

Cashman KV, Sparks RSJ, Blundy JD (2017) Vertically extensive and unstable magmatic systems: a unified view of igneous processes. Science 355:eaag3055

Chalot F, Hughes TJR (1994) A consistent equilibrium chemistry algorithm for hypersonic flows. Comput Methods Appl Mech Eng 112:25–40

Chiodini G, Cioni R, Magro G, Marini L, Panichi C, Raco B, Russo M (1996) Gas and water geochemistry chemical and isotopic variations of Bocca Grande fumarole (Solfatara volcano, Phlegrean Fields). Acta Vulcanol 8:228–232

Chiodini G, Pappalardo L, Aiuppa A, Caliro S (2015) The geological CO_2 degassing history of a long-lived caldera. Geology 43:767–770

Chouet BA, Matoza RS (2013) A multi-decadal view of seismic methods for detecting precursors of magma movement and eruption. J Volcanol Geotherm Res 252:108–175

De Campos CP, Dingwell DB, Perugini D, Civetta L, Fehr TK (2008) Heterogeneities in magma chambers: Insights from the behavior of major and minor elements during mixing experiments with natural alkaline melts. Chem Geol 256:131–145

De Siena L, Del Pezzo E, Bianco F (2010) Seismic attenuation imaging of Campi Flegrei: evidence of gas reservoirs, hydrothermal basins, and feeding systems. J Geophys Res 115:1–18

de Vita S, Orsi G, Civetta L, Carandente A, D'Antonio M, Deino A, Di Cesare T, Di Vito MA, Fisher RV, Isaia R, Marotta E, Necco A, Ort M, Pappalardo L, Piochi M, Southon J (1999) The Agnano-Monte Spina eruption (4100 years BP) in the restless Campi Flegrei caldera (Italy). J Volcanol Geotherm Res 91:269–301

Degruyter W, Huber C (2014) A model for eruption frequency of upper crustal silicic magma chambers. Earth Planet Sci Lett 403:117–130

Di Renzo V, Arienzo I, Civetta L, D'Antonio M, Tonarini S, Di Vito MA, Orsi G (2011) The magmatic feeding system of the Campi Flegrei caldera: architecture and temporal evolution. Chem Geol 281:227–241

Di Renzo V, Wohletz K, Civetta L, Moretti R, Orsi G, Gasparini P (2016) The thermal regime of the Campi Flegrei magmatic system reconstructed through 3D numerical simulations. J Volcanol Geotherm Res 328:210–221

Di Vito M, Isaia R, Orsi G, Southon J, de Vita S, D'Antonio M, Pappalardo L, Piochi M (1999) Volcanism and deformation since 12,000 years at the Campi Flegrei caldera (Italy). J Volcanol Geotherm Res 91:221–246

Flinders J, Clemens JD (1996) Non-linear dynamics, chaos, complexity and enclaves in granitoid magmas. Earth Environ Sci Trans R Soc Edinb 87:217–223

Forni F, Petricca E, Bachmann O, Mollo S, De Astis G, Piochi M (2018) The role of magma mixing/mingling and cumulate melting in the Neapolitan Yellow Tuff caldera-forming eruption (Campi Flegrei, Southern Italy). Contrib Mineral Petrol 173:45

Fourmentraux C, Metrich N, Bertagnini A, Rosi M (2012) Crystal fractionation, magma step ascent, and syn-eruptive mingling: the Averno 2 eruption (Phlegraean Fields, Italy). Contrib Mineral Petrol 163:1121–1137

Garg D, Papale P, Colucci S, Longo A (2019) Long-lived compositional heterogeneities in magma chambers, and implications for volcanic hazard. Sci Rep 9:1–13

Giordano D, Russell JK, Dingwell DB (2008) Viscosity of magmatic liquids: a model. Earth Planet Sci Lett 271:123–134

Gualda GAR, Gravley DM, Deering CD, Ghiorso MS (2019) Magma extraction pressures and the architecture of volcanic plumbing systems. Earth Planet Sci Lett 522:118–124

Hauke G, Hughes TJR (1998) A comparative study of different sets of variables for solving compressible and incompressible flows. Comput Methods Appl Mech Eng 153:1–44

Ishii M, Zuber N (1979) Drag coefficient and relative velocity in bubbly, droplet or particulate flows. AiChE J 25:843–855

Jasim A, Whitaker FF, Rust AC (2015) Impact of channelized flow on temperature distribution and fluid flow in restless calderas: insight from Campi Flegrei caldera, Italy. J Volcanol Geotherm Res 303:157–174

Judenherc S, Zollo A (2004) The Bay of Naples (Southern Italy): constraints on the volcanic structures inferred from a dense seismic survey. J Geophys Res 109: B10312

Kaus BJP, Podladchikov YY (2001) Forward and reverse modeling of the three-dimensional viscous Rayleigh-Taylor instability. Geophys Res Lett 28:1095–1098

Kazahaya K, Shinohara H, Saito G (1994) Excessive degassing of Izu-Oshima volcano: magma convection in a conduit. Bull Volcanol 56:207–216

Lange RA (1994) The effect of H_2O, CO_2 and F on the density and viscosity of silicate melts. Rev Mineral 30:331–369

Longo A, Vassalli M, Papale P, Barsanti M (2006) Numerical simulation of convection and mixing in magma chamber replenished with CO_2-rich magma. Geophys Res Lett 33:L21305

Longo A, Barsanti M, Cassioli A, Papale P (2012a) A finite element Galerkin/least-squares method for computation of multicomponent compressible/incompressible flows. Comput Fluids 67:57–71

Longo A, Papale P, Vassalli M, Saccorotti G, Montagna CP, Cassioli A, Giudice S, Boschi E (2012b) Magma convection and mixing dynamics as a source of ultra-long-period oscillations. Bull Volcanol 74:873–880

Mangiacapra A, Moretti R, Rutherford M, Civetta L, Orsi G, Papale P (2008) The deep magmatic system of the Campi Flegrei caldera (Italy). Geophys Res Lett 35:L21304

Marchetti E, Ichihara M, Ripepe M (2004) Propagation of acoustic waves in a viscoelastic two-phase system: influence of gas bubble concentration. J Volcano Geotherm Res 137:93–108

Masterlark T, Haney M, Dickinson H, Fournier T, Searcy C (2010) Rheologic and structural controls on the deformation of Okmok volcano, Alaska: FEMs, InSAR, and ambient noise tomography. J Geophys Res 115:B02409

Montagna CP, Papale P, Longo A (2015) Timescales of mingling in shallow magmatic reservoirs. Geol Soc London Spec Publ 422:131–140

Montagna CP, Papale P, Longo A, Bagagli M (2017) Magma chamber rejuvenation: insights from numerical models. In Gottsmann J, Neuberg J, Scheu B (eds) Volcanic unrest. Springer, pp 111–122

Moretti R, Arienzo I, Civetta L, Orsi G, Papale P (2013) Multiple magma degassing sources at an explosive volcano. Earth Planet Sci Lett 367:95–104

Morgavi D, Arienzo I, Montagna CP, Perugini D, Dingwell DB (2017) Magma mixing: history and dynamics of an eruption trigger. In Gottsmann J, Neuberg J, Scheu B (eds) Volcanic unrest. Springer, pp 123–137

Oldenburg CM, Spera FJ, Yuen DA, Sewell G (1989) Dynamic mixing in magma bodies: theory, simulations and implications. J Geophys Res 94:9215–9236

Orsi G, D'Antonio M, De Vita S, Gallo G (1992) The Neapolitan Yellow Tuff, a large-magnitude trachytic phreatoplinian eruption: eruptive dynamics, magma withdrawal and caldera collapse. J Volcanol Geotherm Res 53:275–287

Orsi G, de Vita S, di Vito M (1996) The restless, resurgent Campi Flegrei nested caldera (Italy): constraints on its evolution and configuration. J Volcanol Geotherm Res 74:179–214

Orsi G, Petrazzuoli SM, Wohletz K (1999) Mechanical and thermo-fluid behaviour during unrest at the Campi Flegrei caldera (Italy). J Volcanol Geotherm Res 91:453–470

Orsi G, Di Vito MA, Isaia R (2004) Volcanic hazard assessment at the restless Campi Flegrei caldera. Bull Volcanol 66:514–530

Papale P, Moretti R, Barbato D (2006) The compositional dependence of the saturation surface of H_2O+CO_2 fluids in silicate melts. Chem Geol 229:78–95

Papale P, Montagna CP, Longo A (2017) Pressure evolution in shallow magma chambers upon buoyancy-driven replenishment. Geochem Geophys Geosys 18:1214–1224

Pappalardo L, Mastrolorenzo G (2012) Rapid differentiation in a sill-like magma reservoir: a case study from the campi flegrei caldera. Sci Rep 2:712

Parmigiani A, Huber C, Bachmann O (2014) Mush microphysics and the reactivation of crystal-rich magma reservoirs. J Geophys Res-Sol Ea 119:6308–6322

Perugini D, Poli G, Petrelli M, Campos CP, Dingwell DB (2010) Time-scales of recent Phlegrean Fields eruptions inferred from the application of a diffusive fractionation model of trace elements. Bull Volcanol 72:431–447

Perugini D, Poli G (2012) The mixing of magmas in plutonic and volcanic environments: analogies and differences. Lithos 153:61–277

Perugini D, De Campos CP, Petrelli M, Dingwell DB (2015a) Concentration variance decay during magma mixing: a volcanic chronometer. Sci Rep 5:1–10

Perugini D, De Campos CP, Petrelli M, Morgavi D, Vetere FP, Dingwell DB (2015b) Quantifying magma mixing with the Shannon entropy: application to simulations and experiments. Lithos 236–237:299–310

Piochi M, Kilburn CRJ, Di Vito MA, Mormone A, Tramelli A, Troise C, De Natale G (2014) The volcanic and geothermally active Campi Flegrei caldera: an integrated multidisciplinary image of its buried structure. Int J Earth Sci 103:401–421

Pistone M, Blundy J, Brooker RA (2017) Water transfer during magma mixing events: insights into crystal mush rejuvenation and melt extraction processes. Am Mineral 102:766–776

Reid RC, Prausnitz J, Sherwood T (1977) The properties of gases and liquids. McGraw Hill, New York

Ribe NM (1998) Spouting and planform selection in the Rayleigh-Taylor instability of miscible viscous fluids. J Fluid Mech 377:27–45

Roach AC (2005) The evolution of silicic magmatism in the post-caldera volcanism of the Phlegrean Fields, Italy. PhD thesis, Brown University

Ruprecht P, Bergantz GW, Dufek J (2008) Modeling of gas-driven magmatic overturn: tracking of phenocryst dispersal and gathering during magma mixing. Geochem Geophys Geosys 9:Q07017

Schleicher JM, Bergantz GW (2017) The mechanics and temporal evolution of an open-system magmatic intrusion into a crystal-rich magma. J Petrol 58:1059–1072

Seropian G, Rust AC, Sparks RSJ (2018) The gravitational stability of lenses in magma mushes: confined Rayleigh-Taylor instabilities. J Geophys Res-Sol Ea 123:3593–3607

Shakib F, Hughes TJR, Johan Z (1991) A new finite element formulation for computational fluid dynamics: X. The compressible Euler and Navier-Stokes equations. Comput Methods Appl Mech Eng 89:141–219

Sigurdsson H, Houghton BF, McNutt SR, Rymer H, Stix J (2015) The encyclopedia of volcanoes. Elsevier, London, UK, p 1456

Smith VC, Isaia R, Pearce NJG (2011) Tephrostratigraphy and glass compositions of post-15 kyr Campi Flegrei eruptions: implications for eruption history and chronostratigraphic markers. Quat Sci Rev 30:3638–3660

Spera FJ, Yuen DA, Kirschvink SJ (1982) Thermal boundary layer convection in silicic magma chambers: effects of temperature-dependent rheology and implications for thermogravitational chemical fractionation. J Geophy Res 87(B10):8755. https://doi.org/10.1029/JB087iB10p08755

Tamburello G, Caliro S, Chiodini G, De Martino P, Avino R, Minopoli C, Carandente A, Rouwet D, Aiuppa A, Costa A, Bitetto M, Giudice G, Francoforte V, Ricci T, Sciarra A, Bagnato E, Capecchiacci F (2019) Escalating CO_2 degassing at the Pisciarelli fumarolic system, and implications for the ongoing Campi Flegrei unrest. J Volcanol Geotherm Res 384:151–157

Tomlinson EL, Arienzo I, Civetta L, Wulf S, Smith VC, Hardiman M, Lane CS, Carandente A, Orsi G, Rosi M, Müller W, Menzies MA (2012) Geochemistry of the Phlegraean Fields (Italy) proximal sources for major Mediterranean tephras: implications for the dispersal of Plinian and co-ignimbritic components of explosive eruptions. Geochim Cosmochim Acta 93:102–128

Tonarini S, D'Antonio M, Di Vito MA, Orsi G, Carandente A (2009) Geochemical and B-Sr-Nd isotopic evidence for mingling and mixing processes in the magmatic system that fed the Astroni volcano (4.1-3.8 ka) within the Campi Flegrei caldera (Southern Italy). Lithos 107:135–151

Troise C, De Natale G, Schiavone R, Somma R, Moretti R (2019) The Campi Flegrei caldera unrest: discriminating magma intrusions from hydrothermal effects and implications for possible evolution. Earth-Sci Rev 188:108–122

Yoshimura S, Nakamura M (2011) Carbon dioxide transport in crustal magmatic systems. Earth Planet Sci Lett 307:470–478

Zollo A, Maercklin N, Vassallo M, Dello Iacono D, Virieux J, Gasparini P (2008) Seismic reflections reveal a massive melt layer feeding Campi Flegrei caldera. Geophys Res Lett 35(12):L12306. https://doi.org/10.1029/2008GL034242